



HAL
open science

Efficient Pump Photon Recycling via Gain-Assisted Waveguiding Energy Transfer

Roy Aad, Christophe Couteau, Sylvain Blaize, Evelyne Chastaing, Françoise Soyer, Laurent Divay, Christophe Galindo, Pierre Le Barny, Vincent Sallet, Corinne Sartel, et al.

► To cite this version:

Roy Aad, Christophe Couteau, Sylvain Blaize, Evelyne Chastaing, Françoise Soyer, et al.. Efficient Pump Photon Recycling via Gain-Assisted Waveguiding Energy Transfer. ACS photonics, 2014, 1, pp.246 - 253. <10.1021/ph4001179>. <cea-01825676>

HAL Id: cea-01825676

<https://cea.hal.science/cea-01825676v1>

Submitted on 24 Aug 2023

HAL is a multi-disciplinary open access archive for the deposit and dissemination of scientific research documents, whether they are published or not. The documents may come from teaching and research institutions in France or abroad, or from public or private research centers.

L'archive ouverte pluridisciplinaire HAL, est destinée au dépôt et à la diffusion de documents scientifiques de niveau recherche, publiés ou non, émanant des établissements d'enseignement et de recherche français ou étrangers, des laboratoires publics ou privés.



HAL Authorization

Efficient Pump Photon Recycling via Gain-Assisted Waveguiding Energy Transfer

Roy Aad,[†] Christophe Couteau,^{*,†} Sylvain Blaize,[†] Evelyne Chastaing,[‡] Françoise Soyer,[‡] Laurent Divay,[‡] Christophe Galindo,[‡] Pierre Le Barny,[‡] Vincent Sallet,[§] Corinne Sartel,[§] Alain Lussou,[§] Pierre Galtier,[§] Licinio Rocha,^{||} Vesna Simic,^{||} and Gilles Lérondel^{*,†}

[†]Laboratoire de Nanotechnologie et d'Instrumentation Optique (LNIO), Institut Charles Delaunay, CNRS UMR 6281, Université de Technologie de Troyes (UTT), 12 rue Marie Curie, 10010, Troyes France

[‡]Laboratoire de Chimie des Matériaux Organiques, THALES Research and Technology, Campus Polytechnique, 1 avenue Augustin Fresnel, 91767 Palaiseau, France

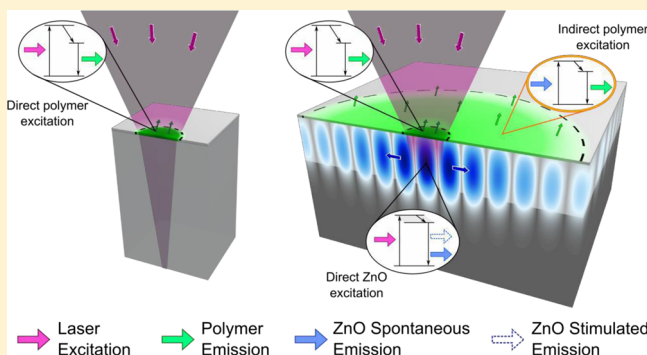
[§]Groupe d'Etude de la Matière Condensée (GEMAC), CNRS-UVSQ, 45 avenue des Etats-Unis, 78035 Versailles, France

^{||}CEA, LIST, Laboratoire Capteurs et Architectures Electroniques, 91191 Gif-sur-Yvette, France

Supporting Information

ABSTRACT: We propose a new concept for enhancing the fluorescence of ultrathin nanolayers. In this article, we address the issue of efficient absorption of polymer thin films with nanometer characteristics. For many applications, such as sensing, but also for lighting or photovoltaics, devices require the use of nanometer-sized films of a specific polymer or a luminescent nanolayer in general. Usually, most studies are geared toward enhancing the emission of such luminescent films via Bragg mirror-type cavities, for instance, but little attention is paid for optimizing the absorption of the thin films. We show the principle of gain-assisted waveguiding energy transfer (G-WET) by inserting a gain-active layer between an active nanometer-scale layer (a luminescent polymer in our case) and the passive substrate. Efficient absorption via “recycling” of the pumping photons is ensured by the waveguiding effect due to this high-index active layer. To demonstrate the G-WET effect, two kinds of samples were studied. They consist of extremely thin (~10 nm) polymer nanolayers spin-coated either on quartz, referred as the passive case, or on a ZnO active thin film (~170 nm, acting as a gain medium) grown on sapphire, referred as the active case. Samples were characterized by room-temperature photoluminescence (PL) spectroscopy under various pumping intensities. Compared to the quartz substrate, the ZnO thin film induces a remarkable enhancement of a factor ~8 on the fluorescence of the polymer nanolayer. Observations show that, for the passive quartz substrate case, the PL of the spin-coated polymer rapidly saturates, defining a luminescence limit; whereas, with the active ZnO layer, the polymer presents a nonlinear PL intensity surpassing the saturation level. This new photonic system revealed that the polymer luminescence enhancement is the result of both an efficient energy transfer and a geometrical effect ensured by an evanescent coupling of the waveguided ZnO stimulated emission. Although our work discusses the specific organic–inorganic case of fluorescent polymer and ZnO, the G-WET concept can be generalized to any hybrid layered sample verifying the necessary energy transfer conditions discussed in this article, thus, demonstrating that this is of a special interest for efficient absorption and efficient recycling of the excitation photons for any nanometer scale fluorescent layer.

KEYWORDS: absorption, emission, ultrathin nanolayer, energy transfer, optical gain, waveguide, fluorescent polymer, zinc oxide



For many applications such as photovoltaic, lighting, lasing, or sensing, efficient absorption and efficient emission of luminescent nanometer-scale layers is desirable. Whereas most of the studies are dedicated to optimize the emission of such layers, very few studies tackle the issue of optimizing the absorption of these fluorescent nanolayers. The best known example is probably a semiconductor quantum well embedded between two highly reflecting Bragg mirrors. In this case, many quantum wells can be embedded within such a structure and

the mirrors provide the feedback and the directionality of the lasing emission in VCSEL for instance.¹ In photovoltaic, efficient absorption is of primary importance. Nowadays, one line of research for optimizing solar cells is to engineer thin efficient absorbers using plasmonics and metamaterials.² Near-perfect absorption was also achieved using graphene² and can

Received: November 11, 2013

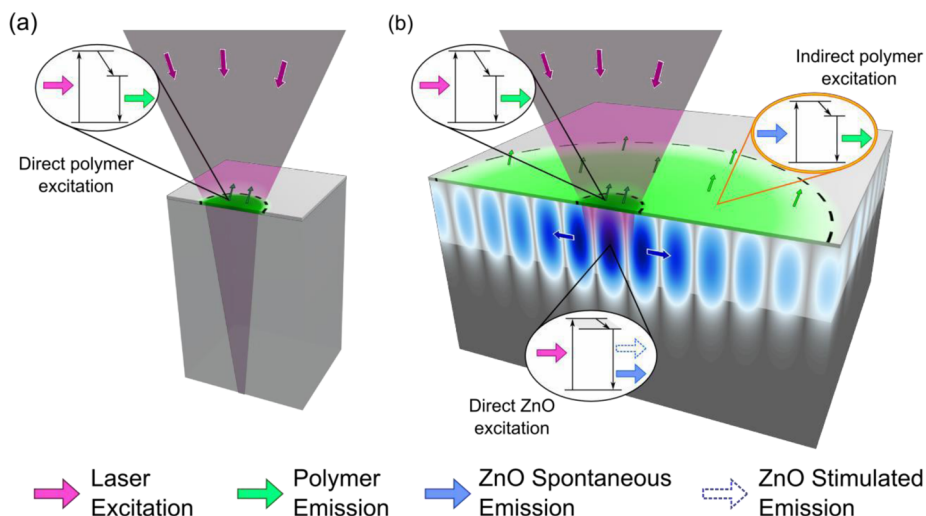


Figure 1. Art picture of the gain-assisted waveguiding energy transfer (G-WET) process for ultrathin film optimized excitation as illustrated for a (polymer) luminescent thin film and an active (ZnO) layer. (a) Case of the passive substrate. A fluorescent polymer layer (light gray) spin-coated on quartz (transparent light blue) is excited by a focused laser beam (transparent violet). The laser spot defines the luminescent polymer area (highlighted in green). The callout bubble represents a brief sketch of the polymer photoluminescence process. (b) Case of the active layer. The fluorescent polymer layer is now spin-coated on ZnO (lighter gray) grown on sapphire (dark gray). A laser beam is again directed toward the structure and excites an equivalent polymer area (limited by the small dashed circle). The laser beam continues toward the ZnO thin film where it is completely absorbed. The ZnO thin film luminesces and preferably couples its emission into a guided mode, represented by the blue guided mode profile. The ZnO guided mode spreads throughout the thin film and repeatedly excites the polymer. Thus, the ZnO excited polymer presents a much larger luminescent area (limited by the large dashed circle). In a similar fashion, the callout bubbles represent the laser (direct) polymer and ZnO excitation and the ZnO (indirect) polymer excitation processes. The dashed blue arrow pictures the stimulated emission.

56 have applications in communications too.³ The idea is to
 57 reduce the absorption layer thickness from few hundreds μm to
 58 submicrometer thickness of silicon or other type of hybrid
 59 semiconductor-metal material. For sensing applications, con-
 60 sidering the thicknesses involved, the cavity configuration is not
 61 possible. Fluorescence quenching polymers have proven to be
 62 potentially interesting materials for achieving highly selective
 63 and extremely sensitive detection of gas molecules in
 64 atmosphere.^{4,5} But the polymer layers are required to be
 65 extremely thin (<20 nm) in order to exhibit fast response times
 66 and low detection thresholds.⁶ The reduction of the polymer
 67 thickness is accompanied by a decrease in the absorption as
 68 well as a decrease in the quantity of fluorescent polymer chains,
 69 which are both responsible for a strong weakening of the
 70 fluorescent intensity of the polymer layer. Thus, the recent
 71 studies on sensing have focused on the fluorescence enhance-
 72 ment of ultrathin polymer nanolayers.

73 The subject of enhancing the fluorescence of emissive
 74 nanometer-size luminescent material was recently tackled by
 75 Rose et al. for sensing applications with polymers.⁷ In this work,
 76 the authors addressed the fluorescence enhancement issue
 77 through a lasing action in the organic polymer layer which
 78 induced a superlinear increase in the polymer fluorescence and
 79 eventually led to a gain in sensitivity. Another related work by
 80 Liu et al. showed that waveguiding within nanowires of
 81 different lengths could select the lasing mode of the nanowire.⁸
 82 This is done by intrinsic self-absorption at the Urbach tail states
 83 of the light emitted from a CdS nanowire. This is another
 84 example of using waveguiding and reabsorption of the pump
 85 photons in order to achieve mode selection. However, no
 86 existing study has yet discussed on enhancing the weak
 87 absorption of the layer rather than optimizing its luminescence.
 88 The issue of very low absorptions remains one of the main
 89 unresolved problems limiting the fluorescence of nanometer
 90 size layers or nanostructures such as nanowires. In this article,

we propose, and later on demonstrate, a new general photonic
 concept of gain assisted waveguiding energy transfer (G-WET)
 for efficient nanothin film luminescence excitation.

Figure 1 presents two 3D illustrations that clarify the
 luminescence excitation issue and the proposed G-WET
 concept. Figure 1a represents the so-called standard case of a
 nanometer thick fluorescent layer (in our case a polymer) on a
 passive (nonemitting) quartz substrate. According to Beer–
 Lambert’s law, ultrathin (<20 nm) polymer layers absorb an
 extremely small percentage of the pumping intensity. As an
 example for the polymer material studied in this article, with an
 absorption coefficient of $7.10^{-4} \text{ nm}^{-1}$ at 337 nm, less than 1.5%
 of the pumping intensity is absorbed. For devices fabricated
 with optically passive supports such as quartz, as illustrated in
 Figure 1a, only a very small amount of the laser excitation (in
 violet) is used to excite the polymer emission (in green) and
 the rest is “wasted” without benefit by going through the
 substrate. Replacing the standard quartz plate with an active
 layer made of a high refractive index material with gain is an
 effective solution to the weak polymer luminescence excitation.
 This active layer is the core of the G-WET phenomenon
 proposed here and illustrated in Figure 1b. In addition to the
 direct excitation by the laser (in violet) leading to an excited
 area defined by the laser spot size (dashed circle), the presence
 of the active layer that can absorb and reemit photons in a
 guided configuration leads to a larger polymer emitting surface
 (larger dashed circle). Let us now describe in more detail the
 different steps of the G-WET process. In order to have an
 optimized energy transfer, the active layer needs to be thick
 enough to absorb all the incident laser intensity as illustrated on
 the figure by the purple gradient. By the same token, to obtain
 an efficient transfer, the active layer luminescence needs to be
 as high as possible and to lie in the polymer absorption range.
 Nonetheless, the energy transfer (ET) process is most efficient
 if it is provided by the evanescent tail of the waveguided modes

126 within the active layer in order to prevent the emitted photons
 127 to escape toward the substrate. The idea is the same when one
 128 wants to pump efficiently nanostructures such as nanowires to
 129 achieve lasing emission. Figure 1b depicts the waveguiding
 130 effect in the active layer with the intensity profile of a guided
 131 mode propagating inside the active layer. With G-WET,
 132 waveguiding is present if the active layer is made of a high
 133 refractive index material. This essential element insures that
 134 guided modes stay strongly confined inside the active layer
 135 (ZnO in our case), subsequently realizing a great number of
 136 round trips within the layer thickness. In this configuration, the
 137 guided mode will repeatedly excite the polymer layer through
 138 the tail of its evanescent wave, which constitutes the most
 139 adequate configuration for an efficient ET process.⁹ The guided
 140 modes spreading throughout the slab can excite polymer chains
 141 lying outside the laser spot, thus, extending the polymer
 142 luminescent surface and inducing a “geometrical” effect. The
 143 active layer thickness therefore should not exceed the limits of a
 144 single-mode waveguide in order to provide the best wave-
 145 guiding configuration. The active layer luminescence must
 146 particularly couple to the fundamental mode which presents the
 147 highest effective index¹⁰ and, in effect, the weakest losses.
 148 Finally, we must stress that another factor is important in our
 149 system. Figure 1b represents the fact that the active layer is a
 150 gain medium which can then show stimulated emission (dashed
 151 blue arrow). This gain factor constitutes the final piece of the
 152 proposed G-WET concept as the stimulated emission amplifies
 153 the luminescence and therefore improves the quantum yield of
 154 the active layer. Equally, this amplified emission improves the
 155 propagation of the guided mode, as the attenuation inside the
 156 active layer is reduced. In the following, we present an
 157 experimental study which demonstrates the previously
 158 discussed G-WET concept by considering the specific case of
 159 ultrathin poly[*dimethyl-co-methyl*-(1,1,1-trifluoro-2-(trifluoro-
 160 methyl)-2-oxy-pent-4-yl)-*co*-(methyl-(4-pentyloxy-(*N*-(2,5-di-
 161 *tert*-butylphenyl))-1,8-naphthalimide)]-siloxane^{11–14} (cf. Sup-
 162 porting Information) called the fluorescent polymer layer later
 163 on. The fluorescent polymer layer is spin-coated on a ZnO film
 164 grown on a sapphire substrate (equivalent to some extent to the
 165 standard quartz substrate by its optical properties).

166 This copolymer was designed to detect nitroaromatic
 167 compounds, more specifically, 2,4-dinitrotoluene and 1,3-
 168 dinitrobenzene¹¹ (chemical compound signatures found in
 169 military grade TNT), by fluorescence quenching of the
 170 fluorescent chromophores located in its side chains. However,
 171 in this paper, this fluorescent polymer was used because it
 172 exhibits an absorption in the 375 nm range which matches with
 173 the peak emission of ZnO. The fluorescent polymer also
 174 exhibits an important Stokes shift (emission peak at 468 nm)
 175 which here allows to clearly separate the two emission
 176 contributions of the fluorescent polymer (ultrathin film) and
 177 the ZnO (active layer).

178 ZnO was chosen as an adequate active support according to
 179 its optical properties. As subsequently detailed, ZnO exhibits a
 180 UV emission^{15–19} that is particularly well-adapted for exciting
 181 the studied polymer layer. Compared to sapphire ($n = 1.8$ at
 182 375 nm) and the polymer ($n = 1.56$ at 375 nm), ZnO has a
 183 high refractive index^{20,21} ($n = 2.57$ at 375 nm) and thus forms
 184 the waveguided layer mentioned earlier. Moreover, stimulated
 185 emission and gain are reported under high pumping
 186 intensities.^{16–19,22–29}

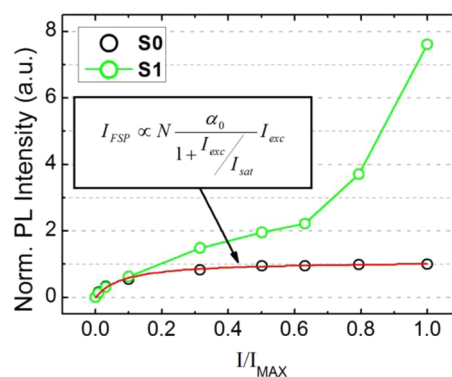
187 Two sets of samples were prepared for this study (Table 1).
 188 The first set (S0) consisted of a polymer nanolayer on quartz

Table 1. List of the Studied Samples

description	sample name	
	S0	S1
polymer nanolayer spin-coated on quartz plates		polymer nanolayer spin-coated on ZnO thin film (~170 nm; cf. Supporting Information)

substrate (used as a reference), while the second set (S1) was
 189 formed by a polymer nanolayer on ZnO film itself grown on
 190 sapphire substrate. To fabricate the samples, a polymer solution
 191 (1.6 mg·mL⁻¹ in methylethyl ketone) was spin-coated on
 192 quartz plates and on ZnO thin films with a spin rate of 3200
 193 rpm for 30 s. Samples were then stored under vacuum at room
 194 temperature to remove the solvent. The spin-coated polymer
 195 formed an 8–10 nm thick nanolayer. ZnO thin films used to
 196 prepare the S1 samples were 170 nm thick and were grown on
 197 R-sapphire by metal–organic chemical vapor deposition
 198 (MOCVD; cf. Supporting Information). Samples were
 199 characterized using room-temperature photoluminescence
 200 (PL) spectroscopy in order to study the impact of the ZnO
 201 thin film on the polymer fluorescence. PL was conducted using
 202 a pulsed nitrogen laser ($\lambda = 337.1$ nm, 4 ns pulse duration)
 203 operating at a repetition rate of 10 Hz. The laser beam was
 204 focused by a lens onto a 1 mm diameter spot with an average
 205 power of 40 μ W. Luminescence was collected using an
 206 objective lens with a 0.13 numerical aperture focused onto a
 207 large core (400 μ m diameter) optical fiber connected to a 50
 208 cm focal length spectrometer equipped with a CCD Peltier-
 209 cooled camera. 210

211 To investigate the influence of the ZnO waveguide, the
 212 polymer fluorescence intensity was measured as a function of
 213 the power using neutral density (ND) filters. Figure 2 shows the



214 Figure 2. Comparison between the photoluminescence of the
 215 fluorescent polymer film coated on quartz, S0 sample (black circles)
 216 and on the ZnO layer, S1 sample (green circles) as a function of the
 217 normalized pumping intensity (I/I_{\max}). The plotted PL intensity values
 218 are taken at $\lambda_{\text{em}}^{\max}$ (~ 468 nm) and normalized by the maximum PL
 219 intensity recorded for the S0 sample.

220 evolution of the PL intensity as a function of the normalized
 221 pumping intensity (I/I_{\max}), for both S0 and S1 samples at 468
 222 nm, which corresponds to the $\lambda_{\text{em}}^{\max}$ of the polymer fluorescence
 223 peak. From hereafter, unless otherwise indicated, all the
 224 presented spectra and PL intensities are normalized by the
 225 maximum $\lambda_{\text{em}}^{\max}$ value presented by S0. Figure 2 reveals a distinct
 226 difference in the polymer fluorescence dependence between the
 227 two samples. 228

For **S0**, the polymer fluorescence (black circles) rapidly saturated and reached a maximum intensity limit as the pumping intensity was increased. The maximum fluorescence is related to the polymer nanolayer thickness and, hence, the number of fluorescent naphthalimide moieties (N) present in the layer. Moreover, the polymer fluorescence behavior can be well described by an absorption saturation³⁰ that subsequently leads to the fluorescence saturation.³¹ The rapid absorption saturation can be attributed to the ultrathin layer thickness (i.e., very small N). Considering a linear fluorescence dependency, the calculated curve fit (black line) can be expressed in the following manner,

$$I_{\text{FSP}} \propto -N \cdot dI/dx = N \cdot \alpha \cdot I_{\text{exc}} = N \frac{\alpha_0}{1 + (I_{\text{exc}}/I_{\text{sat}})} I_{\text{exc}} \quad (1)$$

where α_0 is the polymer absorption coefficient for moderate excitation, N is the number of fluorescent naphthalimide moieties present and I_{FSP} , I_{exc} , and I_{sat} are, respectively, the fluorescent polymer, pumping, and saturation intensities.

On the other hand, for **S1**, the polymer fluorescence (green line) did not saturate even at a high pumping intensity. At low pumping intensities ($I/I_{\text{max}} \leq 0.1$), **S1** presented similar polymer fluorescence levels as **S0**. However, as pumping intensity was further increased, **S1** polymer fluorescence exhibited a superlinear dependency and rapidly exceeded the **S0** values. The fluorescence increase surpassed the saturation limits eventually reaching an up to ~ 8 -fold increase at the maximum pumping intensity. Because the polymer fluorescence presented no saturation tendency, that leaves room for further enhancement with improved experimental conditions. Figure 2 shows the important influence of the ZnO slab on the polymer fluorescence.

In order to understand the origin of the **S1** superlinear increase, it is essential to first verify that this behavior is not an artifact resulting from a spectral overlap between the polymer and a ZnO defect emission. It is therefore important to separately characterize the PL spectrum of the ZnO slab used to fabricate **S1** and, thus, verify if the PL intensity measured at 468 nm (Figure 2) is solely due to the polymer fluorescence. For this purpose, a portion of the **S1** sample was not coated by the polymer in order to measure the ZnO PL. Figure 3 displays the ZnO emission spectrum (dashed black line) along with the

polymer emission (black line) and absorption (blue line) spectra. All the spectra in Figure 3 are normalized by their respective maximum. The collected PL spectrum does not show the presence of ZnO related defect emission. Instead, ZnO manifests a single emission peak in the UV ($\lambda_{\text{em}}^{\text{max}} = 375$ nm) that is widely separated from the polymer fluorescence ($\lambda_{\text{em}}^{\text{max}} = 468$ nm). The wide spectral separation is a favorable aspect for this study, as it prevents unwanted spectral overlapping that can contribute to the collected PL intensity at 468 nm and, therefore, complicate the quantitative analysis of the polymer fluorescence. The emission spectra shown in Figure 3 clearly indicate that the behavior observed for **S1** (as seen in Figure 2) is indeed due to a polymer fluorescence enhancement.

In the meantime, Figure 3 displays another essential feature of the polymer and ZnO layers and an indispensable condition of the proposed concept as it reveals a perfect spectral overlap between the polymer absorption spectrum and the ZnO luminescence spectrum. This spectral “matching” is one of the primary reasons for the choice of ZnO as it insures an efficient polymer excitation (i.e., energy transfer) by the ZnO luminescence. Figure 3 therefore points out to a probable radiative energy transfer that could explain the superlinear polymer fluorescence of **S1**.

In addition to the radiative energy transfer, one can speculate the nonlinear polymer enhancement (seen in Figure 2) to be the result of a stimulated polymer emission, occurring at high pumping intensities. However, it should be clear that this is not the case for the studied polymer. Indeed, if the nonlinear polymer enhancement were due to stimulated emission, then it should have been also observed on **S0**. Furthermore, the occurrence of a stimulated emission can be utterly revoked when looking at the spectral features of the polymer fluorescence. Figure 4 presents the PL spectra of **S0** (a) and **S1** (b), corresponding to the polymer fluorescence intensities shown in Figure 2. As it is seen in Figure 4a,b, the polymer fluorescence presents a constant $\lambda_{\text{em}}^{\text{max}}$ at 468 nm and hardly any change in the full width at half-maximum (fwhm); which ranged between 86 and 90 nm, for the various pumping intensities. However, stimulated emission is normally characterized by a λ_{max} shift and strong narrowing of the fwhm in the luminescence peak. The present polymer fluorescence features exclude the presence of polymer stimulated emission. We would like to point out that nonradiative energy transfer (NRET) processes can also lead to a nonlinear enhancement of the polymer fluorescence. Indeed, NRET processes can occur between organic–inorganic materials.^{32,33} However, these processes are extremely sensitive to donor densities and donor–acceptor coupling and distances. Therefore, NRET processes are more observed between high quality interfaces and for materials presenting a strong exciton confinement at the interface, such as ZnO/ZnMgO quantum wells.^{33,35} This is not the case here, the studied configuration consists of a polymer layer that is spin-coated on a ZnO (170 nm) thin film. Thus, the studied configuration does not present the high quality interface and the strong exciton confinement that are needed to obtain a good NRET efficiency (for a quantitative analysis of the exciton confinement effect in similar system see ref 36). PL measurements realized on a similar polymer layer that was spin-coated on a ZnO thin film but of lower optical quality (i.e., exhibiting no gain or stimulated emission) show no effect on the polymer emission. More precisely, a study of the evolution of the fluorescence intensity as a function of the

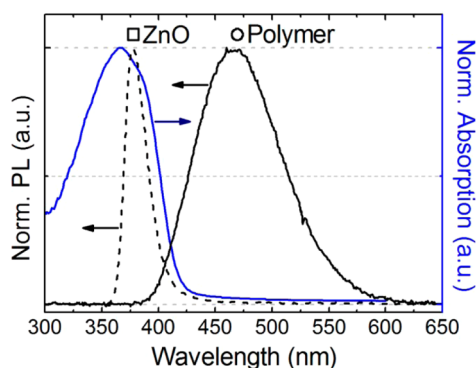


Figure 3. Fluorescence (straight black line) and absorption (straight blue line) spectra of the fluorescent polymer, along with the luminescence spectrum of the ZnO layer (dashed black line). The square and circle, respectively, indicate the ZnO and fluorescent polymer emissions. All presented spectra are normalized to 1, while the arrows mark the corresponding y-axis.

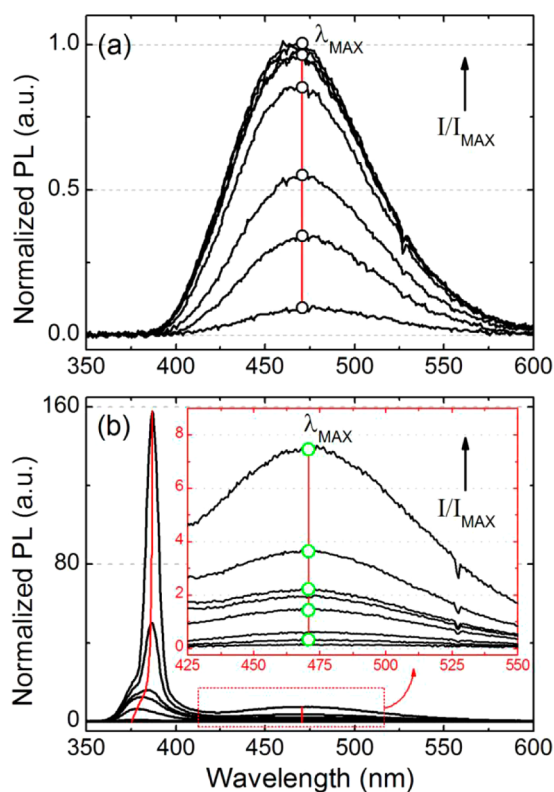


Figure 4. Luminescence spectra of the polymer fluorescent film coated on quartz, S0 sample (a), and on the ZnO layer, S1 sample (b), corresponding to the PL dependency in Figure 2. In analogy, all PL spectra are normalized by the maximum PL intensity recorded for the S0 sample. The red lines show the spectral shift of $\lambda_{\text{em}}^{\text{max}}$ for the various polymer and ZnO luminescence peaks. The presented black (a) and green (b) circles, respectively, indicate the plotted values for the S0 and S1 samples in Figure 2. The arrow in (a) and (b) represent the direction of the ascending I/I_{MAX} . The inset in (b) shows a zoom of the polymer fluorescence.

pumping intensity of the polymer layer deposited on lower optical quality ZnO thin film reveals a similar PL dependency (peak and saturation intensity) to that exhibited by S0 in Figure 2 (study not shown). The latter observation proves that NRET processes are negligible in the studied polymer/ZnO system. However, a study of the PL dynamics, such as in refs 32 and 33, is of need in order to be more quantitative on the contribution of NRET processes in the studied system. However, such a study is beyond the scope of the paper. As shown later in the article, the nonlinear polymer enhancement (cf. Figure 2) is indeed the result of an efficient radiative energy transfer due to the absorption by the polymer thin film of the ZnO waveguided spontaneous amplified emission, that is, evanescent optical coupling.

As previously mentioned, the energy transfer is achieved through the absorption of the ZnO luminescence by the polymer. Hence, investigating the ZnO luminescence can uphold results that further confirm the transfer. Additionally to the polymer fluorescence peak, the S1 spectra presented in Figure 4b show a ZnO related luminescence peak. Contrary to the polymer, the ZnO luminescence exhibited a remarkable change in its spectral features with increasing pumping intensity (indicated by the arrow direction). Under moderate pumping intensities, the ZnO spectra presented a spontaneous excitonic emission peak at $\lambda_{\text{em}}^{\text{max}} \sim 376$ nm with fwhm ~ 23 nm. However,

as the pumping intensity was increased, a new emission peak appeared at the lower energy shoulder ($\lambda_{\text{em}}^{\text{max}} \sim 386$ nm) of the previous peak, which presented a narrowing of the line width (fwhm ~ 9 nm) as well as a behavior with the power excitation suggesting stimulated emission.

By plotting $\lambda_{\text{em}}^{\text{max}}$ in a log–log graph, the power orders of the ZnO luminescence dependency can be determined. Figure 5

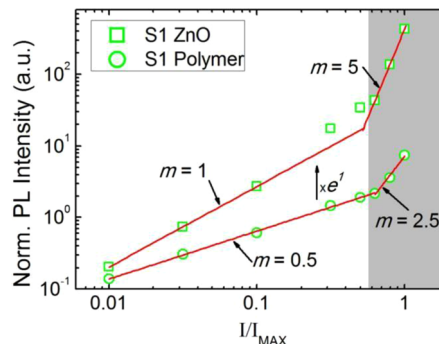


Figure 5. Log–log graph of the PL dependency of the S1 sample with the polymer (green circles) and ZnO (green squares) luminescences as a function of I/I_{MAX} . The red lines show the linear fits. Each of the plotted PL intensity values are taken at the corresponding $\lambda_{\text{em}}^{\text{max}}$ (shown in Figure 4b). The ZnO dependency is multiplied by e^1 to have a better separation from the fluorescent polymer dependency.

presents a log–log plot of the ZnO PL intensity for S1 (green squares) taken at $\lambda_{\text{em}}^{\text{max}}$ (marked by the red line in Figure 4b) for different power excitations. Figure 5 reveals a linear dependency for the first ZnO peak ($\lambda_{\text{em}}^{\text{max}} \sim 376$ nm), collected at low pumping intensities. On the other hand, the second ZnO peak ($\lambda_{\text{em}}^{\text{max}} \sim 386$ nm), appearing at high pumping intensities, manifested a fifth order superlinear increase. The first and second ZnO peaks can be therefore attributed to ZnO excitonic emission (E_{ex} -line) and electron–hole plasma stimulated emission (N-line),^{16,18} respectively.

Furthermore, the polymer fluorescence dependency of S1 (shown in Figure 2) is also plotted in Figure 5 (green circles). Comparing the polymer and ZnO luminescence intensities, Figure 5 shows that a superlinear increase is simultaneously exhibited in both cases. Under moderate pumping intensities, the polymer presented a sublinear fluorescence dependency with a ~ 0.5 order ($I_{\text{FSP}} = I_{\text{exc}}^{0.5}$) typical from a saturation-type power dependence, cf. eq 1. On the other hand, as the ZnO layer passed the stimulated emission threshold, the polymer exhibited a superlinear fluorescence dependency of ~ 2.5 . The sublinear fluorescence dependency suggests that the superlinear fluorescence dependency of the polymer is due to a fifth order excitation ($I_{\text{FSP}} \propto I_{\text{exc}}^{2.5} = (I_{\text{exc}}^S)^{0.5}$), which is precisely the one found for the ZnO active layer case. We can conclude clearly that the superlinear dependencies point out to a strong relation between the polymer fluorescence and the N-line, thus, proving without any doubt the occurrence of an efficient radiative energy transfer. However, the obtained results shown so far neither clarifies the origins of the strong interdependence of the polymer fluorescence to the N-line nor explains how the polymer fluorescence surpasses the saturation limit (cf. Figure 2). For that, as suggested previously, we need to take the waveguiding effect from the active layer into account. Throughout the study, both S0 and S1 samples were excited by the same laser spot ($\varnothing 1$ mm). The laser spot thus defines similar excited volumes of the polymer layer on both samples.

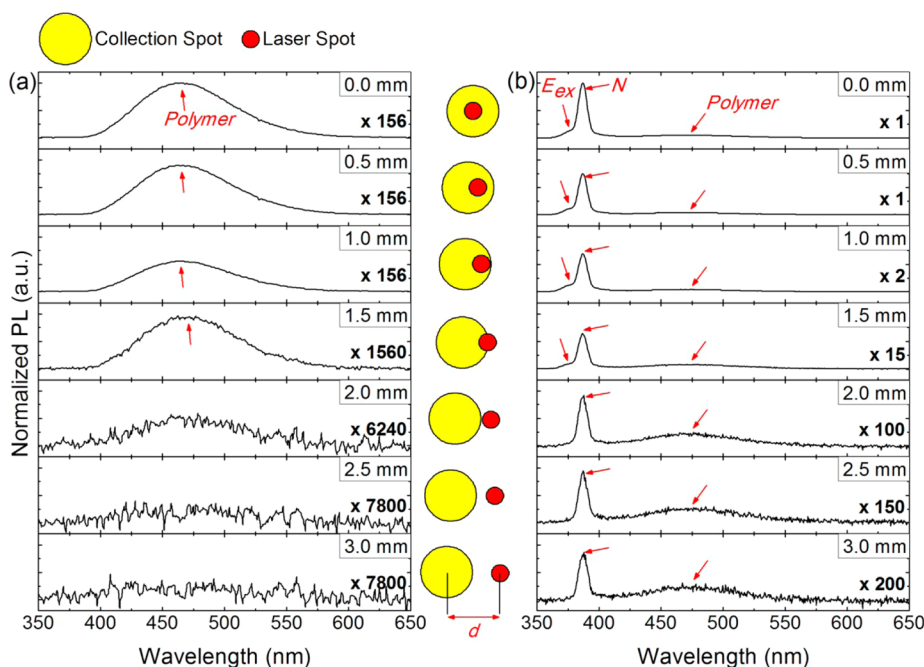


Figure 6. Evolution of the PL spectra for the polymer fluorescent film coated on quartz, **S0** sample (a), and on the ZnO layer, **S1** sample (b), as a function of the distance (d) separating the center laser spot and the axis of the collection objective. The PL spectra are all plotted on the same y-axis scale and normalized by the PL intensity recorded at the $\lambda_{\text{em}}^{\text{max}}$ of the N -line for $d = 0$ mm. The inset between the two figures presents a sketch of the evolution of d .

393 Taking this into consideration, both samples should saturate at
 394 equal polymer fluorescence intensities. Nonetheless, the
 395 polymer fluorescence levels of **S1** appear not to be defined
 396 by the pumped laser volume. This observation suggests the
 397 existence of an additionally excited volume of the polymer due
 398 to a geometrical (i.e., waveguiding) effect.

399 To confirm the presence of a geometrical effect, the
 400 collection lens axis was gradually misaligned in the horizontal
 401 direction, in order to vary the distance d between the lens axis
 402 and the center of the laser spot (inset Figure 6). The PL
 403 measurements were conducted at the highest pumping intensity
 404 (i.e., no neutral density filters were used) in order to provide
 405 the best conditions for obtaining ZnO stimulated emission.
 406 Figure 6 shows the evolution of the **S0** (a) and **S1** (b) spectra
 407 with increasing d (from top to down). Regarding **S0**, Figure 6a
 408 exhibits a polymer fluorescence that gradually decreases as d
 409 increases. Eventually, the fluorescence almost totally diminishes
 410 for $d \geq 2$ mm. At $d = 2$ mm, the collection ($\varnothing \sim 3$ mm) is
 411 tangent to the laser spot ($\varnothing \sim 1$ mm) on the outer side of the
 412 spot. Hence, for **S0**, Figure 6a clearly shows that the excited
 413 polymer area is definitely outside of the laser spot. On the other
 414 hand, regarding **S1**, Figure 6b manifested a polymer and ZnO
 415 luminescence spectra, which also decreased with increasing d
 416 but, in this case, the PL spectra collected outside the laser spot
 417 ($d \geq 2$ mm) still displayed a persisting luminescence.
 418 Compared with **S0**, **S1** clearly presents a much wider
 419 luminescent area. Thus, Figure 6b reveals the existence of a
 420 geometrical effect that clarifies the origins of the **S1** polymer
 421 enhancement. By waveguiding, the excitation area of the
 422 polymer simply increases further than just under the laser spot,
 423 hence, exciting more polymer chains.

424 Furthermore, the ultrathin polymer layer does not support
 425 any guided modes, which means that outside the laser spot (d
 426 ≥ 2 mm), the observed polymer fluorescence is neither guided
 427 in the **S1** structure nor excited by the laser. Clearly, the

observed polymer fluorescence is excited by the evanescent tail 428
 of the ZnO luminescence guided through the slab. On the 429
 other hand, the ZnO layer (170 nm) does constitute an 430
 efficient slab waveguide,^{10,22} and as a consequence, the ZnO 431
 luminescence is mostly coupled into guided modes.³⁷ There- 432
 fore, it is logical to assume that the ZnO luminescence (N -line), 433
 collected for $d \geq 2$ mm, results from guided modes. This 434
 assumption is further confirmed by the evolution of the ZnO 435
 luminescence features observed in Figure 6b. For $d < 2$ mm, 436
 while the collection and laser spots still overlap, Figure 6b 437
 presents a double-peaked ZnO luminescence. The ZnO 438
 luminescence shape results from the overlap of the E_{ex} -line 439
 ($\lambda_{\text{em}}^{\text{max}} \sim 376$ nm) and N -line ($\lambda_{\text{em}}^{\text{max}} \sim 386$ nm). However, as 440
 soon as the collection spot is no longer in coincidence with the 441
 laser spot ($d \geq 2$ mm), Figure 6b shows that only the N -line 442
 remains. Evidently, the E_{ex} -line is only collected from inside the 443
 laser excited surface, while the N -line is collected from both 444
 inside and outside the laser excited surface. This can be 445
 explained easily by the fact that ZnO thin films manifest a 446
 strong and abrupt change in the attenuation coefficient k at the 447
 bandgap (~ 376 nm).^{20,21} Consequently, a small red-shift in the 448
 wavelength, from 376 nm (E_{ex} -line) to 386 nm (N -line), 449
 induces a colossal decrease in k from 0.3 to 0.05,²⁰ respectively. 450
 The E_{ex} -line is therefore strongly attenuated inside the ZnO 451
 slab and is not seen outside the laser spot area. This effect of 452
 reabsorption is well-known in waveguiding in long semi- 453
 conductor nanowires and was observed many times.^{8,38} 454
 Moreover, at 386 nm, the ZnO slab is single mode,¹⁰ and 455
 thus, the N -line is coupled into the fundamental mode, which 456
 leads to its efficient waveguiding throughout the slab. As a 457
 consequence, only the N -line is observable from outside the 458
 laser spot. Figure 6b, thus, demonstrates that the N -line is 459
 solely contributing to the “geometrical” effect discussed 460
 previously. 461

462 To conclude, we presented in this article a new concept to
463 enhance the absorption and therefore the luminescence of
464 ultrathin fluorescent nanolayers for optical applications
465 requiring very thin active layers such as sensing or lasing.
466 Using a gain assisted waveguiding energy transfer (G-WET),
467 we showed that a factor of 8 can be gained for the polymer
468 nanolayer luminescence with our system and, thus, potentially
469 decrease by the same amount the sensing threshold of detectors
470 making use of this effect for instance. We specifically considered
471 the case of fluorescent polymer–ZnO hybrid structures, which
472 consisted of a simple multilayer geometry as planar geometry is
473 easy to fabricate and has the advantage of being homogeneous
474 and rigid. Yet, the fluorescent polymer–ZnO system presents
475 an enhanced luminescence compared to typical samples of
476 polymer on quartz. The experimental investigation revealed the
477 fluorescence enhancement to be the result of an energy transfer
478 and a geometric effect. The geometric effect is shown to be the
479 consequence of guided ZnO stimulated emission as the guided
480 emission propagates along the ZnO thin film and excites a
481 wider polymer nanolayer area. We showed a way to “recycle”
482 laser pumping photons that are usually wasted in the passive
483 substrate. The obtained results validate the proposed concept
484 and show the necessity of using an active waveguiding media as
485 support. In general, we think that the G-WET method allows
486 one to lower the pumping level of the excitation photons,
487 provided that an active layer with particular properties (right
488 thickness, matching absorption, waveguiding, gain medium) is
489 inserted between the fluorescent nanolayer and the passive
490 substrate. In an ultimate approach, the G-WET concept can
491 eventually be combined with nanostructured active layers such
492 as 2D photonic crystals or self-formed cavities that can present
493 reduced lasing threshold due to dielectric confinement, as
494 recently demonstrated in ref 39. This concept goes beyond the
495 presented structure of fluorescent polymer and ZnO and can be
496 used for other hybrid structures.

497 ■ ASSOCIATED CONTENT

498 ● Supporting Information

499 Information concerning the synthesis of the fluorescent
500 polymer and the growth of the ZnO thin film. This material
501 is available free of charge via the Internet at <http://pubs.acs.org>.

502 ■ AUTHOR INFORMATION

503 Corresponding Author

504 *E-mail: couteau@utt.fr; lerondel@utt.fr.

505 Notes

506 The authors declare no competing financial interest.

507 ■ ACKNOWLEDGMENTS

508 This work was supported by the ANR Project ULTRAFLU and
509 the CPER Project MATISSE. One of the authors, R.A., would
510 like to thank the Champagne-Ardenne regional council for the
511 Ph.D. support. The authors would also like to thank Loïc LE
512 CUNFF for his help in preparing the figures.

513 ■ REFERENCES

- 514 (1) Peters, F.; Peters, M.; Young, D.; Thibeault, B.; Corzine, S.;
515 Coldren, L. High-Power Vertical-Cavity Surface-Emitting Laser. *Elec.*
516 *Lett.* **1993**, *29*, 200–201.
517 (2) Atwater, H. A.; Polman, A. Plasmonics for Improved Photovoltaic
518 Devices. *Nat. Mater.* **2010**, *9*, 205–213.
519 (3) Zhang, J.; MacDonald, K. F.; Zheludev, N. I. Controlling Light-
520 with-Light without Nonlinearity. *Light Sci. Appl.* **2012**, *1*, e18.

- (4) Melinte, V.; Buruiana, T.; Tampu, D.; Buruiana, E. C. Synthesis
of Hybrid Nanocomposites Based on New Triazeno Copolymers and
Montmorillonite Used for Detecting Metal Ions. *Polym. Int.* **2011**, *60*,
102–111.
(5) Sinha, J.; Kumar, A. Syntheses and Characterization of Amplified
Fluorescence Poly(aryleneethynylene)s Based on 3,4-Propylenedioxy-
thiophenes and Their Application in TNT Sensing. *Synth. Met.* **2010**,
160, 2265–2272.
(6) Yang, J.-S.; Swager, T. M. Fluorescent Porous Polymer Films as
TNT Chemosensors: Electronic and Structural Effects. *J. Am. Chem.*
530 *Soc.* **1998**, *120*, 11864–11873.
(7) Rose, A.; Zhu, Z.; Madigan, C. F.; Swager, T. M.; Bulovic, V.
Sensitivity Gains in Chemosensing by Lasing Action in Organic
533 Polymers. *Nature* **2005**, *434*, 876–879.
(8) Liu, X.; Zhang, Q.; Xiong, Q.; Sum, T. C. Tailoring the Lasing
535 Modes in Semiconductor Nanowire Cavities Using Intrinsic Self-
536 Absorption. *Nano Lett.* **2013**, *13*, 1080–1085.
(9) Aad, R.; Blaize, S.; Bruyant, A.; Couteau, C.; Léronnel, G.
538 Enhancement of Ultra-Thin Film Emission Using a Waveguiding
539 Active Layer. *J. Appl. Phys.* **2010**, *108*, 123111–7.
(10) Yariv, A.; Yeh, P. *Photonics*, 6th ed.; Oxford University Press:
541 New York, 2006.
(11) Le Barny, P.; Obert, E.; Soyer, F.; Malval, J. P.; Leray, I.;
543 Lemaitre, N.; Pansu, R.; Simic, V.; Doyle, H.; Redmond G.; Loiseaux,
544 B. Detection of Nitroaromatic Compounds Based on Photo-
545 luminescent Side Chain Polymers. *SPIE Proc.* **2005**, vol. 5990.
(12) Bojino, V.; Grabchev, I. A New Method for Synthesis of 4-
547 Allyloxy-1,8-naphthalimide Derivatives for Use as Fluorescent Bright-
548 eners. *Dyes Pigm.* **2001**, *51*, 57–61.
(13) Ghorbanian, S.; Tyman, J.; Tychopoulos, V. J. The Synthesis of
550 Symmetrical and Unsymmetrical Alkylaminonaphthalic-1,8-N-alkyl-
551 imides. *Chem. Technol. Biotechnol.* **2000**, *75*, 1127–1134.
(14) Hamel, M.; Simic, V.; Normand, S. Fluorescent 1,8-
553 Naphthalimides-Containing Polymers as Plastic Scintillators. An
554 Attempt for Neutron–Gamma Discrimination. *React. Funct. Polym.*
555 **2008**, *68*, 1671–1681.
(15) Tang, Z. K.; Wong, G. K. L.; Yu, P.; Kawasaki, M.; Ohtomo, A.;
557 Koinuma, H.; Segawa, Y. Room-Temperature Ultraviolet Laser
558 Emission from Self-Assembled ZnO Microcrystallite Thin Films.
559 *Appl. Phys. Lett.* **1998**, *72*, 3270–3272.
(16) Tang, Z. K.; Kawasaki, M.; Ohtomo, A.; Koinuma, H.; Segawa,
561 Y. Self-Assembled ZnO Nanocrystals and Exciton Lasing at Room
562 Temperature. *J. Cryst. Growth* **2006**, *287*, 169–179.
(17) Zu, P.; Tang, Z. K.; Wong, G. K. L.; Kawasaki, M.; Ohtomo, A.;
564 Koinuma, H.; Segawa, Y. Ultraviolet Spontaneous and Stimulated
565 Emissions from ZnO Microcrystallite Thin Films at Room Temper-
566 ature. *Solid State Commun.* **1997**, *103*, 459–463.
(18) Kawasaki, M.; Ohtomo, A.; Ohkubo, I.; Koinuma, H.; Tang, Z.
568 K.; Yu, P.; Wong, G. K. L.; Zhang, B. P.; Segawa, Y. Excitonic
569 Ultraviolet Laser Emission at Room Temperature from Naturally
570 Made Cavity in ZnO Nanocrystal Thin Films. *Mater. Sci. Eng., B* **1998**,
571 *56*, 239–244.
(19) Segawa, Y.; Ohtomo, A.; Kawasaki, M.; Koinuma, H.; Tang, Z.
573 K.; Yu, P.; Wong, G. K. L. Growth of ZnO Thin Film by Laser MBE:
574 Lasing of Exciton at Room Temperature. *Phys. Status Solidi B* **1997**,
575 *202*, 669–672.
(20) Postava, K.; Sueki, H.; Aoyama, M.; Yamaguchi, T.; Ino, Ch.;
577 Igasaki, Y.; Horie, M. Spectroscopic Ellipsometry of Epitaxial ZnO
578 Layer on Sapphire Substrate. *J. Appl. Phys.* **2000**, *87*, 7820–7824.
(21) Yoshikawa, H.; Adachi, S. Optical Constants of ZnO. *Jpn. J.*
580 *Appl. Phys.* **1997**, *36*, 6237–6243.
(22) Yu, P.; Tang, Z. K.; Wong, G. K. L.; Kawasaki, M.; Ohtomo, A.;
582 Koinuma, H.; Segawa, Y. Room-Temperature Gain Spectra and Lasing
583 in Microcrystalline ZnO Thin Films. *J. Cryst. Growth* **1998**, *184*, 601–
584 605.
(23) Reynolds, D. C.; Look, D. C.; Jogai, B. Optically pumped
586 ultraviolet lasing from ZnO. *Solid State Commun.* **1996**, *99*, 873–875.
587

- 588 (24) Bagnall, D. M.; Chen, Y. F.; Zhu, Z.; Yao, T.; Koyama, S.; Shen,
589 M. Y.; Goto, T. Optically Pumped Lasing of ZnO at Room
590 Temperature. *Appl. Phys. Lett.* **1997**, *70*, 2230–2232.
- 591 (25) Chen, Y.; Tuan, N. T.; Segawa, Y.; Ko, H.-J.; Hong, S.-K.; Yao,
592 T. Stimulated Emission and Optical Gain in ZnO Epilayers Grown by
593 Plasma-Assisted Molecular-Beam Epitaxy with Buffers. *Appl. Phys. Lett.*
594 **2001**, *78*, 1469–1471.
- 595 (26) Divay, L.; Rogers, D. J.; Lusso, A.; Kostcheev, S.; Mc Murtry,
596 S.; Léronnel, G.; Hosseini Téhérani, F. Studies of Optical Emission in
597 the High Intensity Pumping Regime of Top-down ZnO Nanostruc-
598 tures and Thin Films Grown on c-Sapphire Substrates by Pulsed Laser
599 Deposition. *Phys. Status Solidi C* **2008**, *5*, 3095–3097.
- 600 (27) Cao, H.; Zhao, Y. G.; Ong, H. C.; Ho, S. T.; Dai, J. Y.; Wu, J. Y.;
601 Chang, R. P. H. Ultraviolet Lasing in Resonators Formed by Scattering
602 in Semiconductor Polycrystalline Films. *Appl. Phys. Lett.* **1998**, *73*,
603 3656–3658.
- 604 (28) Cao, H.; Zhao, Y. G.; Ho, S. T.; Seelig, E. W.; Wang, Q. H.;
605 Chang, R. P. H. Random Laser Action in Semiconductor Powder. *Phys.*
606 *Rev. Lett.* **1999**, *82*, 2278–2281.
- 607 (29) Dupont, P.-H.; Couteau, C.; Rogers, D. J.; Hosseini Téhérani,
608 F.; Léronnel, G. Waveguiding-Assisted Random Lasing in Epitaxial
609 ZnO Thin Film. *Appl. Phys. Lett.* **2010**, *97*, 261109–3.
- 610 (30) Svelto, O.; Hanna, D. C. *Principles of Lasers*, 4th ed.; Plenum
611 Press: New York, 1998.
- 612 (31) Schroeder, R.; Ullrich, B. Absorption and Subsequent Emission
613 Saturation of Two-Photon Excited Materials: Theory and Experiment.
614 *Opt. Lett.* **2002**, *27*, 1285–1287.
- 615 (32) Coakley, K. M.; McGehee, M. D. Conjugated Polymer
616 Photovoltaic Cells. *Chem. Mater.* **2004**, *16*, 4533–4542.
- 617 (33) Blumstengel, S.; Sadofev, S.; Puls, J.; Henneberger, F. An
618 Inorganic/Organic Semiconductor “Sandwich” Structure Grown by
619 Molecular Beam Epitaxy. *Adv. Mater.* **2009**, *21*, 4850–4853.
- 620 (34) Nguyen, H. M.; Seitz, O.; Aureau, D.; Sra, A.; Nijem, A.;
621 Gartstein, Y. N.; Chabal, Y. J.; Malko, A. V. Spectroscopic Evidence for
622 Nonradiative Energy Transfer between Colloidal CdSe/ZnS Nano-
623 crystals and Functionalized Silicon Substrates. *Appl. Phys. Lett.* **2011**,
624 *98*, 161904–3.
- 625 (35) Nimmo, M. T.; Caillard, L. M.; De Benedetti, W.; Nguyen, H.
626 M.; Seitz, O.; Garstein, Y. N.; Chabal, Y. J.; Malko, A. V. Visible to
627 Near-Infrared Sensitization of Silicon Substrates via Energy Transfer
628 from Proximal Nanocrystals: Further Insights for Hybrid Photo-
629 voltaics. *ACS Nano* **2013**, *7*, 3236–3245.
- 630 (36) Aad, R.; Simic, V.; Le Cunff, L.; Rocha, L.; Sallet, V.; Sartet, C.;
631 Lusso, A.; Couteau, C.; Léronnel, G. ZnO Nanowires As Effective
632 Luminescent Sensing Materials for Nitroaromatic Derivatives. *Nano-*
633 *scale* **2013**, *5*, 9176–9180.
- 634 (37) Benisty, H.; Stanley, R.; Mayer, M. Method of Source Terms for
635 Dipole Emission Modification in Modes of Arbitrary Planar Structures.
636 *J. Opt. Soc. Am. A* **1998**, *15*, 1192–1201.
- 637 (38) Duan, X.; Huang, Y.; Agarwal, R.; Lieber, C. M. Single-
638 Nanowire Electrically Driven Lasers. *Nature* **2003**, *421*, 241–245.
- 639 (39) Chen, R.; Ling, B.; Sun, X. W.; Sun, H. D. Room Temperature
640 Excitonic Whispering Gallery Mode Lasing from High-Quality
641 Hexagonal ZnO Microdisks. *Adv. Mater.* **2011**, *23*, 2199–2204.